

Alfvénic fluctuations in “newborn” polar solar wind

B. Bavassano¹, E. Pietropaolo², and R. Bruno¹

¹Istituto di Fisica dello Spazio Interplanetario, Istituto Nazionale di Astrofisica, Rome, Italy

²Dipartimento di Fisica, Università di L’Aquila, L’Aquila, Italy

Received: 27 January 2005 – Revised: 30 March 2005 – Accepted: 5 April 2005 – Published: 3 June 2005

Abstract. The 3-D structure of the solar wind is strongly dependent upon the Sun’s activity cycle. At low solar activity a bimodal structure is dominant, with a fast and uniform flow at the high latitudes, and slow and variable flows at low latitudes. Around solar maximum, in sharp contrast, variable flows are observed at all latitudes. This last kind of pattern, however, is a relatively short-lived feature, and quite soon after solar maximum the polar wind tends to regain its role. The plasma parameter distributions for these newborn polar flows appear very similar to those typically observed in polar wind at low solar activity. The point addressed here is about polar wind fluctuations. As is well known, the low-solar-activity polar wind is characterized by a strong flow of Alfvénic fluctuations. Does this hold for the new polar flows too? An answer to this question is given here through a comparative statistical analysis on parameters such as total energy, cross helicity, and residual energy, that are of general use to describe the Alfvénic character of fluctuations. Our results indicate that the main features of the Alfvénic fluctuations observed in low-solar-activity polar wind have been quickly recovered in the new polar flows developed shortly after solar maximum.

Keywords. Interplanetary physics (MHD waves and turbulence; Sources of the solar wind) – Space plasma physics (Turbulence)

1 Introduction

The 3-D structure of the solar wind dramatically changes during the Sun’s activity cycle. This feature, first seen in wind speed values estimated from interplanetary scintillation observations (e.g. Rickett and Coles, 1983), has been unambiguously confirmed by in-situ measurements of Ulysses, the first spacecraft able to perform an almost complete latitudinal scan (about $\pm 80^\circ$) of the heliosphere. From the beginning

of its journey away from the ecliptic plane in February 1992, through a Jupiter gravity assist, Ulysses has performed observations for more than an entire solar activity cycle, with two full out-of-ecliptic orbits completed in mid-2004. From this huge data set it comes out very clearly that at low solar activity the solar wind has quite a simple bimodal structure, with a fast, tenuous, and uniform flow filling large angular sectors at high heliographic latitudes (the so-called polar wind) and slower, more variable, and highly structured flows at low latitudes (e.g. McComas et al., 1998, 2000). Around solar maximum, in sharp contrast, variable flows are observed at all latitudes and the wind structure appears to be a complicated mixture of flows coming from a variety of sources (McComas et al., 2002, 2003). However, this kind of wind pattern persists for a relatively short fraction of the high-solar-activity phase. For the remainder of the cycle a bimodal structure is the dominant feature of the 3-D solar wind.

All this is well illustrated by Figs. 1 and 2, referring to the first and the second out-of-ecliptic orbit of Ulysses, respectively. The latitudinal variation of the wind velocity is displayed in the top polar graphs, with time running anticlockwise from the left arrow. Note that the angular resolution is variable, with a maximum at the aphelion (left) and a minimum at the perihelion (right), due to changes in the Ulysses angular velocity along the orbit. A bimodal structure is clearly apparent in Fig. 1, where data from day 48 (1992), just after the Jupiter flyby, to day 346 (1997) are plotted. As shown by the sunspot number vs. time curve in the bottom panel, this interval, highlighted as a thick segment, covers the entire descending phase of a cycle (cycle 22) and the beginning of the next one. Conversely, a bimodal structure is not seen in Fig. 2 (top panel), covering days from 347 (1997) to 51 (2004). This interval includes (see thick segment in the bottom panel) the rising phase of cycle 23, its maximum, and the beginning of its descending phase. A first striking feature of Fig. 2 is the absence of persistent fast wind during the Southern Hemisphere crossing, occurring when the solar cycle attains its highest levels. A second remarkable point is that at the next polar crossing in

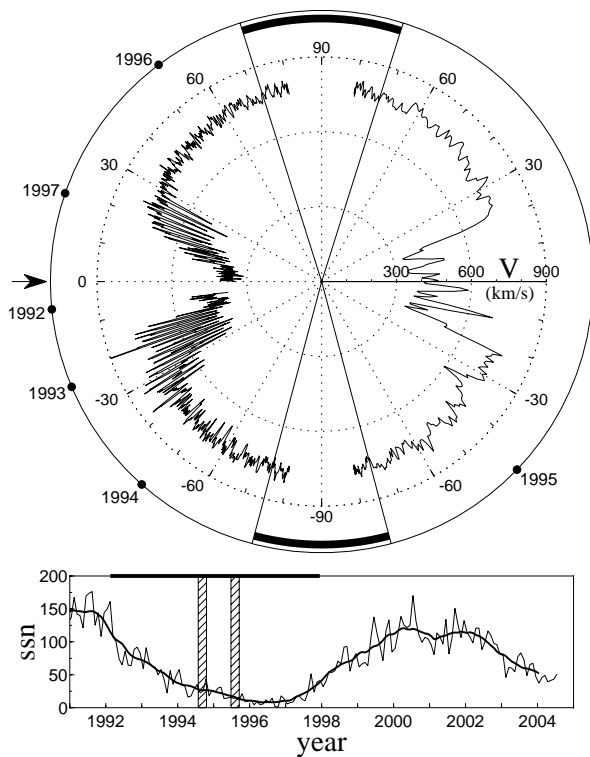


Fig. 1. Top: Solar wind velocity V (daily averages) vs. heliographic latitude as observed by Ulysses during days from 48 (1992) to 346 (1997). Dots along the outermost circle mark the beginning of each year, with time increasing anticlockwise starting from the arrow on the left. Bottom: Solar sunspot numbers (ssn) vs. time starting from 1991. Monthly and smoothed values are plotted as a thin and a thick line, respectively. A thick segment on top marks the time interval of the data displayed in the polar V panel.

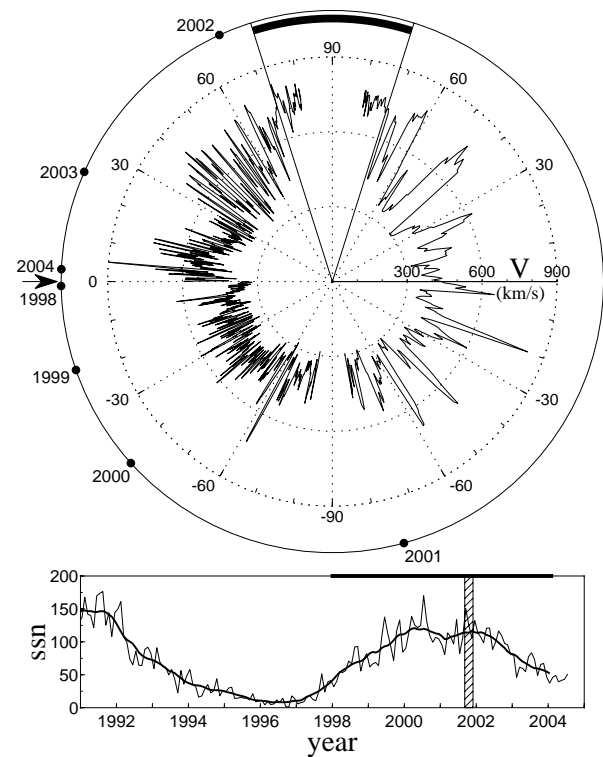


Fig. 2. Solar wind velocity vs. latitude as observed by Ulysses during days from 347 (1997) to 51 (2004), in the same format of Fig. 1.

the Northern Hemisphere, less than one year later but after the solar magnetic field reversal (Jones et al., 2003), the situation has greatly changed, with an extended high-latitude sector of wind with speed well above 600 km/s. McComas et al. (2002) have shown that these post-maximum fast flows are virtually indistinguishable (in terms of statistical distributions of plasma parameters as velocity, density, temperature, and alpha-particle abundance) from the polar flows observed by Ulysses during its first orbit. In other words, at the time of the second orbit northern crossing, the polar wind rebuilding is already well under way. This reflects the restructuring of the solar magnetic field after its reversal phase, with a re-growing of the northern polar coronal hole (e.g. Miralles et al., 2001).

As is well known, an outstanding feature of the low-solar-activity polar wind is that of a strong and ubiquitous flow of Alfvénic fluctuations, largely dominant with respect to all other kinds of perturbation (see, e.g. Goldstein et al., 1995; Horbury et al., 1995; Smith et al., 1995). The point that we will address here is: Does this hold for the new after-maximum polar flows too? In other words, does the Alfvénic

regime quickly recover its features, as is seen to occur for plasma conditions? The aim of the present investigation is to answer to this question.

It is worth recalling that Alfvénic fluctuations in solar wind are usually a mixture of two different populations, characterized by an opposite direction of propagation in the wind plasma frame of reference. The first population, dominant in the great majority of cases, is made up of fluctuations propagating, in the wind frame, away from Sun (outward population), while the second population is made up of fluctuations propagating, in the wind frame, towards the Sun (inward population). Obviously, outside the Alfvénic critical point (where the solar wind becomes super-Alfvénic), both kinds of fluctuation are convected outwards, as seen from the Sun. The major source for outward fluctuations seen in the interplanetary space is the Sun, with smaller contributions from interplanetary sources. Conversely, interplanetary inward fluctuations can only come from sources in regions outside the Alfvénic critical point (in fact, inside this point inward waves fall back to the Sun). As is well known (e.g. Dobrowolny et al., 1980), the presence of the two kinds of waves is a condition that leads to the development of nonlinear interactions.

Though Ulysses observations have offered a new perspective to solar wind studies, many fundamental advances in understanding the behaviour of Alfvénic fluctuations date back from the seventies and eighties, with spacecraft

measurements confined within a small latitudinal belt around the solar equator. This was made possible by the fact that near-equator fast streams, coming from equatorward extensions of polar coronal holes (or small low-latitude holes), are rich in Alfvénic fluctuations. For an exhaustive review on the results in the near-equator wind, reference can be made to Tu and Marsch (1995). Discussions of the Ulysses observations in polar wind, with comparisons to low-latitude results, can be found in Goldstein et al. (1995), Horbury and Tsurutani (2001), and Bavassano et al. (2004).

2 Data and method of analysis

The data used in the present study are those of the solar wind plasma and magnetic field experiments aboard the Ulysses spacecraft (principal investigators D. J. McComas and A. Balogh, respectively), as made available by the World Data Center A for Rockets and Satellites (NASA Goddard Space Flight Center). The plasma data are the fluid velocity vector (averaged over proton and alpha-particle populations), the proton number density, the alpha-particle number density, and the proton temperature. The time resolution of plasma measurements is either 4 or 8 min, depending on the spacecraft mode of operation. The magnetic data are 1-minute averages of higher resolution measurements.

The computational scheme of our analysis is quite simple. For each plasma velocity vector \mathbf{V} we first compute the corresponding magnetic field vector \mathbf{B} by averaging over 4 (or 8) min, then derive the Elsässer’s variables, defined as (Elsässer, 1950)

$$\mathbf{Z}_{\pm} = \mathbf{V} \pm \mathbf{B}/\sqrt{4\pi\rho}, \quad (1)$$

where ρ is the mass density. A discussion on the use of Elsässer variables in studies on solar wind fluctuations may be found in the review of Tu and Marsch (1995). These variables are ideally suited to separately identify Alfvénic fluctuations propagating in opposite directions. When studying Alfvénic fluctuations in solar wind, it is useful to know that \mathbf{Z}_{+} fluctuations always correspond to outward modes and \mathbf{Z}_{-} fluctuations to inward modes, regardless of the background magnetic field direction. This request is fulfilled if Eq. (1) is used for a background field with a sunward component along the local spiral direction, while for the opposite magnetic polarity the equation

$$\mathbf{Z}_{\pm} = \mathbf{V} \mp \mathbf{B}/\sqrt{4\pi\rho} \quad (2)$$

is taken. In the following we will apply this dual definition. Obviously, in the case of folded (or S-shaped) field configurations, erroneous outward/inward classifications are obtained. This, however, occurs for quite a small number of cases (see Balogh et al., 1999).

Once the time series of the Elsässer variables \mathbf{Z}_{+} and \mathbf{Z}_{-} are obtained, their total variances, e_{+} and e_{-} , as given by the trace of their variance matrix, are computed. The values of e_{+} and e_{-} give a measure of the energy per unit mass associated with \mathbf{Z}_{+} and \mathbf{Z}_{-} fluctuations in a given frequency

Table 1. The analysed data intervals: start and end times (year, day, hour), minimum and maximum distances (R , in AU), and latitudes (λ , in degrees, with n and s for north and south, respectively).

interval	time	R		λ	
		min	max	min	max
LS	94 209 17 – 94 292 20	2.03	– 2.61	75.1s	– 80.2s
LN	95 176 13 – 95 260 17	1.77	– 2.36	72.5n	– 80.2n
HN	01 248 12 – 01 332 16	1.77	– 2.35	72.5n	– 80.2n

band, determined by the data sampling time (see above) and by the averaging time used to evaluate variances. Results discussed here refer to hourly variances. This choice is based on the well-established result (e.g. see Tu and Marsch, 1995) that fluctuations on an hourly scale fall in the core of the inertial ($f^{-5/3}$) Alfvénic regime (see Goldstein et al., 1995, and Horbury et al., 1995). Shorter intervals would have too small a number of data points, while longer intervals would include contributions from low frequencies outside the inertial regime.

In addition to e_{+} and e_{-} , two other quantities will be used to describe Alfvénic fluctuations, namely the normalized cross-helicity, σ_C , and the normalized residual energy, σ_R (for a discussion on these quantities, see Matthaeus and Goldstein, 1982, and Roberts et al., 1987a). They are defined as $\sigma_C = (e_{+} - e_{-}) / (e_{+} + e_{-})$ and $\sigma_R = (e_V - e_B) / (e_V + e_B)$, with e_V and e_B the energies (per unit mass) of \mathbf{V} and $\mathbf{B}/\sqrt{4\pi\rho}$ fluctuations, respectively, as given by their total variances (at hourly scale in the present case). Both parameters may only vary between -1 and $+1$. The cross-helicity σ_C gives a measure of the energy balance between the two components (outward and inward) of the Alfvénic fluctuations. The value of σ_C is 1 (-1) when only the outward (inward) component is present. Absolute values of σ_C below 1 correspond to a mixture of the two components and/or to the presence of non-Alfvénic variations in the solar wind parameters. The residual energy σ_R gives the balance between kinetic and magnetic energy (with the magnetic field scaled to Alfvén units through the factor $1/\sqrt{4\pi\rho}$). The absence of magnetic (kinetic) fluctuations corresponds to σ_R equal to $+1$ (-1), while equipartition gives $\sigma_R = 0$. It should finally be recalled that σ_C and σ_R have to fulfill the constraint $\sigma_C^2 + \sigma_R^2 \leq 1$ (provided that $\sigma_R \neq \pm 1$, see Bavassano et al., 1998).

3 The investigated intervals and their Alfvénic content

Our analysis is based on a comparison between fluctuations in post-maximum polar wind and in low-activity polar wind from the point of view of their Alfvénic character. An inspection of the post-maximum flows observed by Ulysses in the Northern Hemisphere during its second orbit (Fig. 2) has allowed one to identify at the highest latitudes an interval of three solar rotations (as seen by Ulysses) in which polar wind conditions appear to be well established. We have decided to

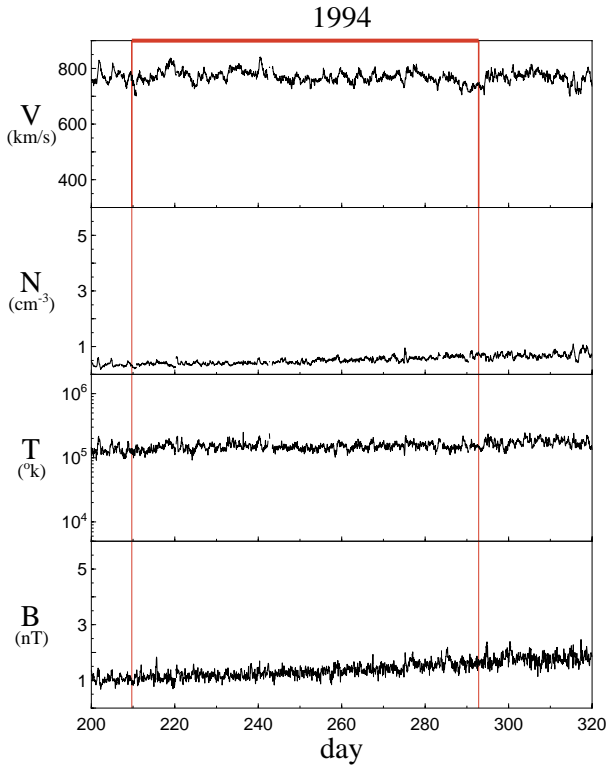


Fig. 3. Hourly averages of the solar wind velocity V , the proton number density N , the proton temperature T , and the magnetic field magnitude B vs. time at the southern polar pass of the Ulysses first out-of-ecliptic orbit. Red lines indicate the interval that corresponds to the three southernmost solar rotations (label LS in Table 1).

study the Alfvénic content of this interval and to compare it to that found for analogous (in terms of latitude and duration) intervals in low-activity polar wind.

The selected intervals are listed in Table 1, identified by a two-letter label (the first letter gives the solar activity level, L=low and H=high, the second letter is for the hemisphere, N=north and S=south). Intervals labeled LS and LN refer to the first Ulysses orbit, with LS for the southern polar crossing in 1994 and LN for the northern one in 1995, both at low solar activity. They have already been the object of past studies on Alfvénic fluctuations (e.g. see Goldstein et al., 1995; Smith et al. 1995; and Bavassano et al., 2000a, b). The third interval, labeled HN, is for the 2001 northern crossing at high solar activity. These intervals are highlighted as thick angular sectors and dashed bands in Fig. 1 (LS and LN, around the South and North pole, respectively) and Fig. 2 (HN, around the North pole).

Hourly averages of the solar wind plasma (protons plus alpha particles) velocity, the proton number density, the proton temperature, and the magnetic field magnitude for the investigated intervals are shown in Figs. 3, 4, and 5 (between red lines). The 1994 and 1995 intervals correspond to very stable and almost identical wind conditions. The situation is not exactly the same for the newborn polar wind of the 2001 interval. Here, even though a fast wind appears well established

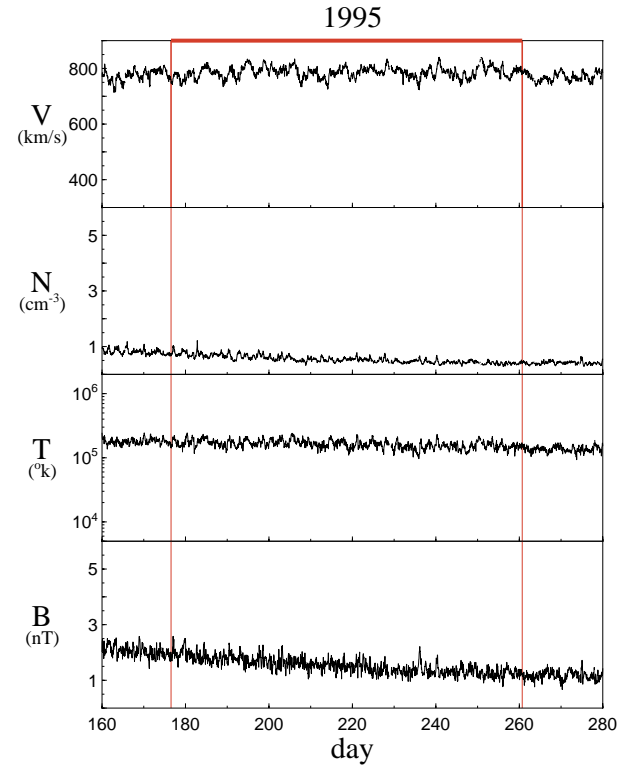


Fig. 4. Solar wind parameters at the northern polar pass of the Ulysses first out-of-ecliptic orbit, in the same format of Fig. 3. Red lines indicate the interval that corresponds to the three northernmost solar rotations (label LN in Table 1).

(see McComas et al., 2002), flow conditions are not as steady as for the 1994 and 1995 intervals, and several velocity gradients are observed. Though weak in comparison to those seen in low-latitude wind, these gradients represent non negligible perturbations of the polar flow, with the development of compression/rarefaction regions. However, it clearly appears from Fig. 5 that the 2001 sample has extended periods during which the wind is relatively steady (see blue lines).

As discussed above, our analysis is based on the computation of hourly values of e_+ , e_- , σ_C , and σ_R . In addition to this, to evaluate the level of variations of compressive type, hourly standard deviations of the magnetic field magnitude (s_B) and the proton density (s_N), normalized to B and N hourly values, have been computed. Time plots of this set of parameters for the investigated intervals in 1994, 1995, and 2001 are shown in Figs. 6, 7, and 8, respectively.

The data shown in Figs. 6 and 7 are from the data set used by Bavassano et al. (2000a, b). As already well discussed (see also Goldstein et al., 1995), these low-solar-activity polar samples are characterized by an Alfvénic flow dominated by the outward fluctuations component, as easily seen from the displacement of σ_C towards high positive values. Moreover, as is typical for observations outside ~ 1 AU (e.g. see Matthaeus and Goldstein, 1982, and Roberts et al., 1987a), an imbalance of σ_R towards negative values (i.e. larger amplitudes of magnetic field fluctuations with respect

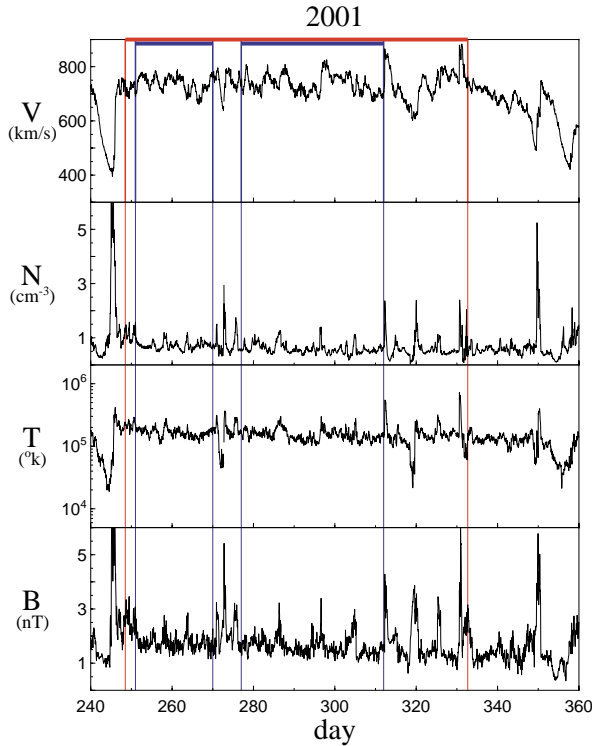


Fig. 5. Solar wind parameters at the northern polar pass of the Ulysses second out-of-ecliptic orbit, in the same format of Fig. 3. Red lines indicate the three northernmost rotations interval (label HN in Table 1). Blue lines mark periods in which the wind is relatively steadier (see text).

to velocity fluctuations) is clearly apparent. All this occurs in the presence of low values of s_B and s_N , below 0.1 for the large majority of cases.

Are these features observed in the 2001 newborn polar wind too? An answer can come from a comparison of Figs. 6 and 7 to Fig. 8, where the results for the 2001 interval are shown. As already mentioned above, flow conditions for this interval are less steady than for the 1994 and 1995 intervals, and this is expected to affect the Alfvénic fluctuation properties (e.g. see Roberts et al., 1987b, 1992). Velocity gradient effects are certainly present in the Fig. 8 data, with a decrease of σ_C and an increase of σ_R , s_B , and s_N . However, if we focus on the intervals between blue lines, where (see above) the irregularities in the wind velocity are of lesser relevance, appreciable differences with respect to low-activity results (Figs. 6 and 7) do not come out. Thus, the Alfvénic character appears to have been quickly recovered in the post-maximum polar wind.

4 The σ_C - σ_R and e_+ - e_- pairs

To further compare the 2001 interval Alfvénic features with those of the 1994 and 1995 intervals, an occurrence frequency analysis of the values of σ_C , σ_R , e_+ , and e_- has been performed. More specifically, 2-D histograms of the

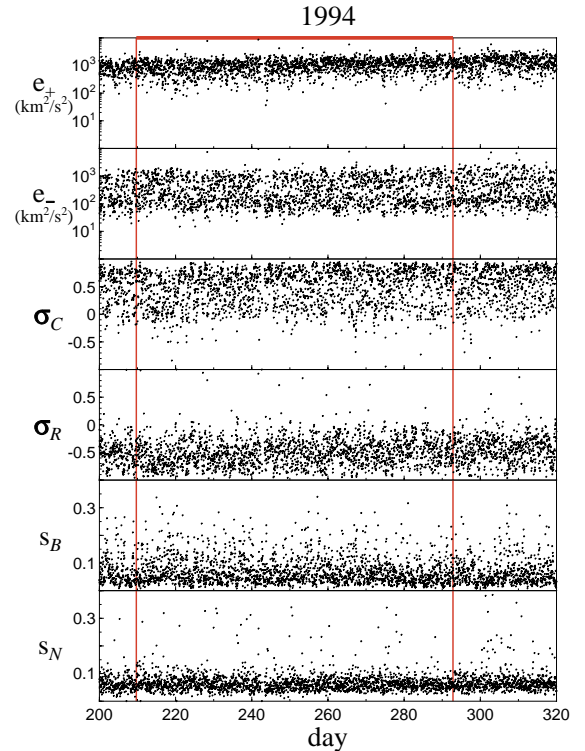


Fig. 6. From top to bottom, hourly values of e_+ , e_- , σ_C , σ_R , s_B , and s_N are plotted vs. time for the 1994 polar interval (LS).

parameter pairs σ_C - σ_R and e_+ - e_- have been derived for the three intervals. For 2001 data the analysis has been performed for both the whole interval and the subintervals delimited by blue lines in Fig. 8. The histograms are shown as coloured contour plots in the panels of Figs. 9 and 10. A label in the upper left corner indicates the examined interval (2001* is for the 2001 blue-line subintervals).

Histograms of Fig. 9 indicate that the Ulysses observations tend to cluster in the bottom right quadrant, where σ_C is positive and σ_R negative. Following the constraint $\sigma_C^2 + \sigma_R^2 \leq 1$, the σ_C - σ_R pairs fall inside a circle of radius 1, drawn in red in the four panels (the small blue areas outside the circle are the effect of interpolations in constructing the coloured surface graphs). It is worth recalling (Bavassano et al., 1998) that the correlation coefficient between \mathbf{V} and $\mathbf{B}/\sqrt{4\pi\rho}$ fluctuations is closer to 1 (in absolute value) the closer to the unit circle the corresponding σ_C - σ_R pair falls.

A great similarity exists between the four distributions of Fig. 9. In all cases a prominent peak emerges at $\sigma_C \sim 0.8$ and $\sigma_R \sim -0.5$, in the proximity of the unit circle (i.e. for highly correlated velocity and magnetic fluctuations). It is accompanied by a tail extending towards $\sigma_C \sim 0$ and $\sigma_R \sim -1$, with a weak secondary peak at the end. The main peak is easily interpreted in terms of wind regions dominated by \mathbf{Z}_+ fluctuations. Not surprisingly, for the 2001* subset this feature emerges in a cleaner way than for the whole 2001 sample. The secondary peak corresponds to cases for which magnetic fluctuations exist nearly in the absence of velocity

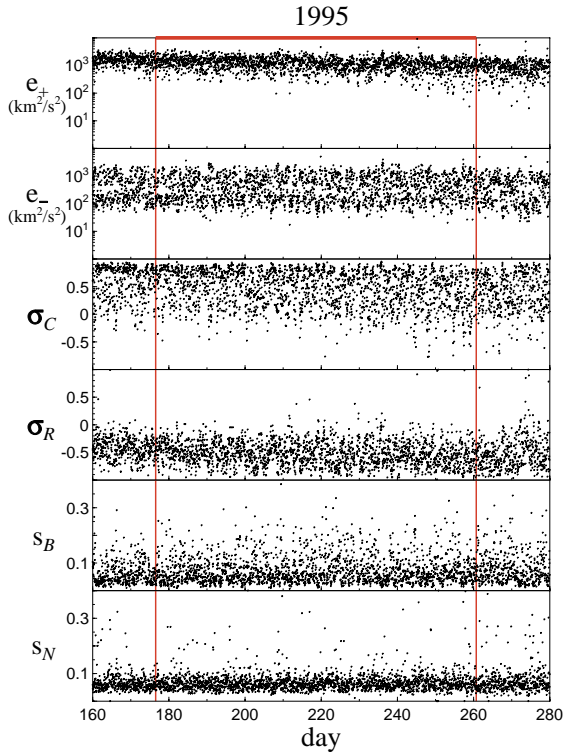


Fig. 7. Hourly values of e_+ , e_- , σ_C , σ_R , S_B , and S_N vs. time for the 1995 polar interval (LN).

fluctuations. Similar cases were observed in the inner heliosphere by Tu and Marsch (1991), who interpreted them as a special type of convected magnetic structures. Thus, histograms of Fig. 9 indicate that the polar wind fluctuations essentially are a mixture of Alfvénic fluctuations and convected structures of magnetic type (see also Bavassano et al., 1998). This is a support to models (e.g. Tu and Marsch, 1993) based on a superposition of such two components.

The frequency distributions shown in Fig. 10 indicate that also for the Z_+ and Z_- fluctuation energies essentially the same pattern is observed in the different samples. The great majority of points falls within a narrow band close to the $e_+=10e_-$ line (white solid line). The e_+-e_- pairs of this band represent the Alfvénic population typically found in the polar wind, with a largely dominant contribution from outgoing fluctuations, and correspond to the main peak at $\sigma_C \sim 0.8$ seen in Fig. 9 (σ_C is 0.82 for $e_+/e_-=10$). The remaining points mostly fall in the region between the band and the $e_+=e_-$ line (white dashed line). As is obvious, the $e_+ \sim e_-$ cases of Fig. 10 correspond to the $\sigma_C \sim 0$ cases of Fig. 9. It is worth mentioning that the e_+ values in the main band tend to be higher for the 1995 interval. This could be an effect of the lower level of variability that characterizes the wind seen by Ulysses during the northern polar pass in 1995, as compared to other polar wind phases (e.g. see Bavassano et al., 2005).

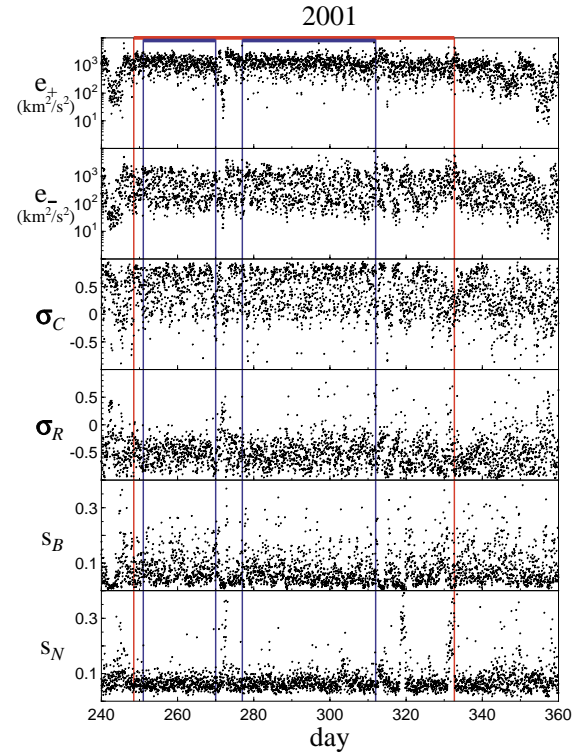


Fig. 8. Hourly values of e_+ , e_- , σ_C , σ_R , S_B , and S_N vs. time for the 2001 polar interval (HN). Blue lines mark wind regions relatively unaffected by velocity gradient effects.

5 Summary and conclusion

The dependence of the 3-D structure of the solar wind on the Sun’s activity cycle, first seen in wind speed values estimated from interplanetary scintillation, has been unambiguously confirmed by in-situ measurements of Ulysses, the first spacecraft able to perform an almost complete latitudinal scan of the heliosphere. At low solar activity a bimodal structure is dominant, with a fast and uniform flow at high latitudes, and slow and variable flows at low latitudes. Around solar maximum, in sharp contrast, variable flows are observed at all latitudes. This last kind of pattern, however, has a relatively short life. In fact, quite soon after solar maximum the fast high-latitude wind is seen to regain its role, though solar activity remains high (see Fig. 2).

From statistical distributions of the Ulysses measurements McComas et al. (2002) have concluded that the 2001 newborn polar flows exhibit plasma features (as velocity, density, temperature, and alpha-particle abundance) virtually indistinguishable from those typical of the low-solar-activity polar wind. However, when time profiles of wind velocity, density, temperature, and magnetic field are examined for the intervals investigated here (see Figs. 3 to 5), flow conditions in 2001 do not appear to be as steady as in 1994 and 1995. Though weak in comparison to gradients seen in low-latitude wind, the velocity variations observed in the 2001 sample represent non negligible perturbations in the plasma flow,

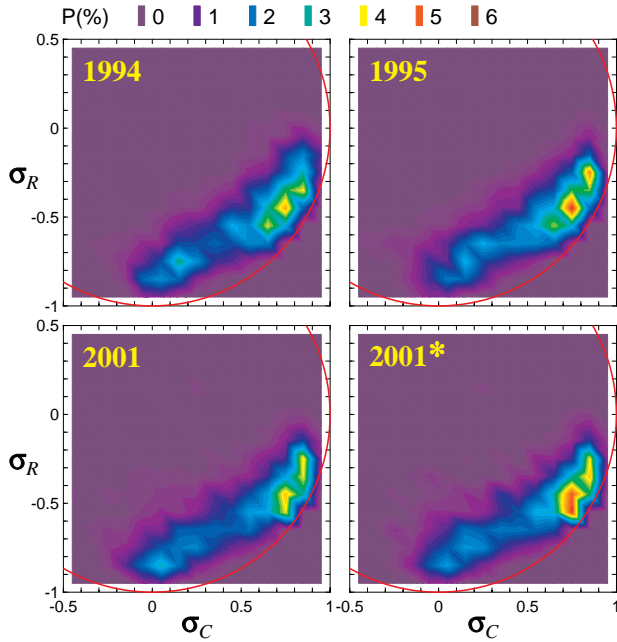


Fig. 9. Occurrence frequency distributions of the σ_C - σ_R pairs are shown in the four panels, with the label in the upper left corner to indicate the interval under examination. The 2001* panel is for the subintervals of the 2001 sample (highlighted by the blue lines in Figs. 5 and 8). The colour code for the occurrence frequency P (in per cent) is shown on top. The red circle indicates the limit value for the sum of σ_C^2 and σ_R^2 (see text).

with clear evidence of compression and rarefaction effects.

The point addressed in the present paper is about a relevant feature of the low-activity polar wind, namely the ubiquitous presence of a strong flow of Alfvénic fluctuations. Does this remain valid for the post-maximum polar wind too?

In order to obtain an answer to this question we have determined for the post-maximum polar flow seen in 2001 the values of the parameters that are generally used to characterize fluctuations of Alfvénic type (namely Z_+ and Z_- fluctuation energies, normalized cross-helicity, and normalized residual energy) and have compared them with those obtained for low-activity polar wind intervals in 1994 and 1995 (already investigated by Bavassano et al., 2000a, b). From this comparison (e.g. see Figs. 9 and 10) it clearly appears that significant differences between the examined samples for the values of e_+ , e_- , σ_C , and σ_R do not come out. Thus, though the plasma flow for the post-maximum polar interval is not as steady as for those at low solar activity, the Alfvénic character of the fluctuations clearly appears to be essentially the same.

In conclusion, the main features of the flow of Alfvénic fluctuations typical of the low-activity polar wind are fully recovered in the newborn polar streams seen shortly after the solar maximum.

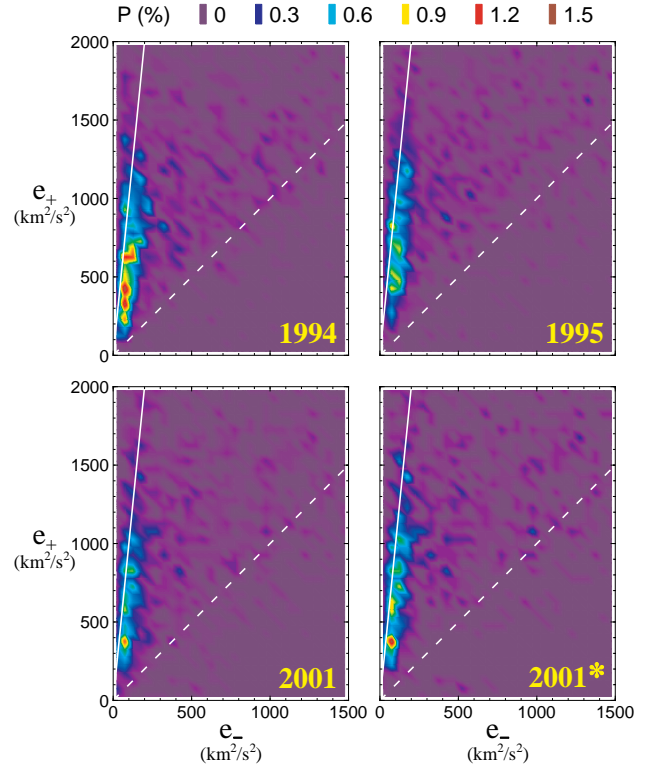


Fig. 10. Fluctuation energies are shown in terms of occurrence frequency distributions in the e_+ - e_- plane. The four panels have the same meaning as in Fig. 9. The colour code for the occurrence frequency P (in per cent) is shown on top. White lines are for $e_+ = 10e_-$ (solid) and $e_+ = e_-$ (dashed).

Acknowledgements. The use of data of the plasma analyzer (principal investigator D. J. McComas, Southwest Research Institute, San Antonio, Texas, USA) and of the magnetometers (principal investigator A. Balogh, The Blackett Laboratory, Imperial College, London, UK) aboard the Ulysses spacecraft is gratefully acknowledged. The data have been made available through the World Data Center A for Rockets and Satellites (NASA/GSFC, Greenbelt, Maryland, USA). Solar sunspot data are from the World Data Center for the Sunspot Index, Royal Observatory of Belgium (Brussels, Belgium).

Topical Editor R. Forsyth thanks M. L. Goldstein and another referee for their help in evaluating this paper.

References

- Balogh, A., Forsyth, R. J., Lucek, E. A., and Horbury, T. S.: Heliospheric magnetic field polarity inversions at high heliographic latitudes, *Geophys. Res. Lett.*, 26, 631–634, 1999.
- Bavassano, B., Bruno, R., and Carbone, V.: MHD Turbulence in the Heliosphere, in: *The Sun and the heliosphere as an integrated system*, edited by Poletto, G. and Suess, S. T., Kluwer Academic Publishers, Dordrecht, The Netherlands, Astrophysics and Space Science Library, v. 317, 253–281, 2004.
- Bavassano, B., Bruno, R., and D’Amicis, R.: Large-scale velocity fluctuations in polar solar wind, *Ann. Geophys.*, 23, 1025–1031, 2005, [SRef-ID: 1432-0576/ag/2005-23-1025](#).

- Bavassano, B., Pietropaolo, E., and Bruno, R.: Cross-helicity and residual energy in solar wind turbulence: radial evolution and latitudinal dependence in the region from 1 to 5 AU, *J. Geophys. Res.*, 103, 6521–6529, 1998.
- Bavassano, B., Pietropaolo, E., and Bruno, R.: Alfvénic turbulence in the polar wind: A statistical study on cross helicity and residual energy variations, *J. Geophys. Res.*, 105, 12 697–12 704, 2000a.
- Bavassano, B., Pietropaolo, E., and Bruno, R.: On the evolution of outward and inward Alfvénic fluctuations in the polar wind, *J. Geophys. Res.*, 105, 15 959–15 964, 2000b.
- Dobrowolny, M., Mangeney, A., and Veltri, P.: Properties of magnetohydrodynamic turbulence in the solar wind, *Astron. Astrophys.*, 83, 26–32, 1980.
- Elsässer, W. M.: The hydromagnetic equations, *Phys. Rev.*, 79, 183–183, 1950.
- Goldstein, B. E., Smith, E. J., Balogh, A., Horbury, T. S., Goldstein, M. L., and Roberts, D. A.: Properties of magnetohydrodynamic turbulence in the solar wind as observed by Ulysses at high heliographic latitudes, *Geophys. Res. Lett.*, 22, 3393–3396, 1995.
- Horbury, T. S., Balogh, A., Forsyth, R. J., and Smith, E. J.: Observations of evolving turbulence in the polar solar wind, *Geophys. Res. Lett.*, 22, 3401–3404, 1995.
- Horbury, T. S. and Tsurutani, B. T.: Ulysses measurements of waves, turbulence and discontinuities, in: *The heliosphere near solar minimum: The Ulysses perspective*, edited by: Balogh, A., Marsden, R. G., and Smith, E. J., Springer-Praxis Books in Astrophysics and Astronomy, London, UK, ISBN 1-85233-204-2, 167–227, 2001.
- Jones, G. H., Balogh, A., and Smith, E. J.: Solar magnetic field reversal as seen at Ulysses, *Geophys. Res. Lett.*, 30(19), 8028, doi:10.1029/2003GL017204, 2003.
- Matthaeus, W. H. and Goldstein, M. L.: Measurement of the rugged invariants of magnetohydrodynamic turbulence in the solar wind, *J. Geophys. Res.*, 87, 6011–6028, 1982.
- McComas, D. J., Bame, S. J., Barraclough, B. L., Feldman, W. C., Funsten, H. O., Gosling, J. T., Riley, P., Skoug, R., Balogh, A., Forsyth, R., Goldstein, B. E., and Neugebauer, M.: Ulysses return to the slow solar wind, *Geophys. Res. Lett.*, 25, 1–4, 1998.
- McComas, D. J., Barraclough, B. L., Funsten, H. O., Gosling, J. T., Santiago-Muñoz, E., Skoug, R. M., Goldstein, B. E., Neugebauer, M., Riley, P., and Balogh, A.: Solar wind observations over Ulysses first full polar orbit, *J. Geophys. Res.*, 105, 10 419–10 433, 2000.
- McComas, D. J., Elliot, H. A., Gosling, J. T., Reisenfeld, D. B., Skoug, R. M., Goldstein, B. E., Neugebauer, M., and Balogh, A.: Ulysses’ second fast-latitude scan: Complexity near solar maximum and the reformation of polar coronal holes, *Geophys. Res. Lett.*, 29(9), doi:10.1029/2001GL014164, 2002.
- McComas, D. J., Elliott, H. A., Schwadron, N. A., Gosling, J. T., Skoug, R. M., and Goldstein, B. E.: The three-dimensional solar wind around solar maximum, *Geophys. Res. Lett.*, 30(10), 1517, doi:10.1029/2003GL017136, 2003.
- Miralles, M. P., Cranmer, S. R., and Kohl, J. L.: UVCS observations of a high-latitude coronal hole with high oxygen temperatures and the next solar cycle polarity, *Ap. J.*, 560, L193–L196, 2001.
- Rickett, B. J. and Coles, W. A.: Solar cycle evolution of the solar wind in three dimensions, *Proceedings of Solar Wind 5 Conference*, edited by: Neugebauer, M., NASA Conference Publication 2280, 315–321, 1983.
- Roberts, D. A., Klein, L. W., Goldstein, M. L., and Matthaeus, W. H.: The nature and evolution of magnetohydrodynamic fluctuations in the solar wind: Voyager observations, *J. Geophys. Res.*, 92, 11 021–11 040, 1987a.
- Roberts, D. A., Goldstein, M. L., Klein, L. W., and Matthaeus, W. H.: Origin and evolution of fluctuations in the solar wind: Helios observations and Helios-Voyager comparisons, *J. Geophys. Res.*, 92, 12 023–12 035, 1987b.
- Roberts, D. A., Goldstein, M. L., Matthaeus, W. H., and Ghosh, S.: Velocity shear generation of solar wind turbulence, *J. Geophys. Res.*, 97, 17 115–17 130, 1992.
- Smith, E. J., Balogh, A., Neugebauer, M., and McComas, D. J.: Ulysses observations of Alfvén waves in the southern and northern solar hemispheres, *Geophys. Res. Lett.*, 22, 3381–3384, 1995.
- Tu, C.-Y. and Marsch, E.: A case study of very low cross-helicity fluctuations in the solar wind, *Ann. Geophys.*, 9, 319–332, 1991.
- Tu, C.-Y. and Marsch, E.: A model of solar wind fluctuations with two components: Alfvén waves and convective structures, *J. Geophys. Res.*, 98, 1257–1276, 1993.
- Tu, C.-Y. and Marsch, E.: MHD structures, waves and turbulence in the solar wind: Observations and theories, *Space Sci. Rev.*, 73, 1–210, 1995.